Research Article

Journal of Environmental Nanotechnology

Biodiesel Synthesis over Mesoporous Solid Acid Catalyst

S. Senthurselvi, M. Krishnaveni, C. Kannan*

Department of Chemistry, Manonmaniam Sundaranar University, Tirunelveli, TN, India

Received: 21.08.2019 Accepted: 25.09.2019 Published: 30-09-2019

*chellapandiankannan@gmail.com

ABSTRACT

A simple and new hydrothermal method was adopted to synthesize $CuAlPO_4$ and $MgAlPO_4$ catalysts by using Triethylamine as a template. The synthesized catalysts were characterized by using FT-IR, XRD, SEM and BET. These characterization techniques have proved the formation of tetrahedral frameworks of $CuAlPO_4$ and $MgAlPO_4$ catalysts. The biodiesel synthesis reaction has been carried out with ethanol. The experimental conditions like contact time, temperature, mole ratio and catalyst dosage were optimized for maximum conversion. Conversion of biodiesel and selectivity of biodiesel was more on $CuAlPO_4$ than $MgAlPO_4$.

Keywords: Biodiesel; Characterization; New technique; Solid acid.

1. INTRODUCTION

Biodiesel is an alternative source in the petroleum fuel field. It can be used in a diesel engine without much changes. Easy biodegradability of biodiesel is also one of its benefits. Generally, biodiesel is less poisonous compared to ordinary diesel. Therefore, in current years, research depends on plant-based fuels. Different plant-based oils have been involved in biodiesel syntheses, such as canola, Jatropha, palm kernel, sunflower and palm (Wilson, 2007). Catalysts used in biodiesel synthesis, such as homogeneous and heterogenous were reported in the literature (Subrahmanyam *et al.* 2003). Research has been done based on the application of heterogeneous catalysts to produce biodiesel because of the eco-friendly and economic benefits (Elangovan *et al.* 1998). The surfactant molecules were used as important templates in the production of meso-structured molecular sieves with the cubic or hexagonal ordering of the pore system (Tatsuo Kimura, 2005). Moreover, the surfactant molecules caused environmental pollution and corrosion (Jing Yu *et al.* 2007). To solve all these problems, a beneficial and eco-friendly attempt has been made to produce mesoporous aluminophosphate molecular sieves with the minimum expense (Selvam and Mohapatra, 2006). In the recent investigation, $AlPO_4$-based heterogeneous catalysts were applied for transesterification reaction. For this purpose, a new nanoporous solid acid $AlPO_4$ has been prepared by using triethylamine as a template. The triethylamine was reported for the preparation of microporous $AlPO_4$-based materials (Cheralathan *et al.* 2000). In the present investigation, triethylamine was used to prepare mesoporous aluminophosphate molecular sieve by adopting a simple hydrothermal method without using the autoclave.

2. EXPERIMENTAL METHODOLOGY

2.1 Materials

The chemicals for the synthesis of mesoporous aluminophosphate were aluminium hydroxide and phosphoric acid; the metal sulphates utilized for the isomorphous substitution in the $AlPO_4$ framework were $MgSO_4$ and $CuSO_4$ respectively. Castor oil and ethanol were employed for the transesterification reaction. The catalysts used for the reaction were $MgAlPO_4$ and $CuAlPO_4$.

2.2 Methods

Mesoporous aluminophosphate was prepared by using triethylamine as a template by a simple synthesis method with the following gel composition: $0.98Al_2O_3$: P_2O_5:0.02MO:$(C_2H_5)_3N$:$300H_2O$. 7.8 g of aluminium hydroxide was dissolved in 7 ml of water and added slowly into the template (triethylamine) solution and stirred for 1 h. Phosphoric acid was dissolved with 25 ml of water. Then $CuSO_4$ and $MgSO_4$ were added for two separate syntheses of $CuAlPO_4$ and $MgAlPO_4$. The concentration of metal ion was 0.02 M, and was added to the above mixture and stirred continuously for 2 h to achieve a homogenous mixture. Then the resulting gel was heated and dried in the hot plate at 120 °C in the open air and thoroughly washed with de-ionized water. The solid was then filtered, dried and calcinated at 400 °C for 6 h to remove the organic template.

2.3 Characterization

Various techniques have been used for the characterization of $AlPO_4$, including FT-IR, XRD, surface area and pore size distribution and SEM. Fourier Transform Infrared (FTIR) spectra of mesoporous $AlPO_4$ were recorded in a Jasco FTIR-41° spectrophotometer in the range of 4000-400 cm^{-1} using KBr pellet techniques. The formation of mesoporous in $AlPO_4$-based molecular sieves was studied by powder XRD. X-ray Diffraction (XRD) patterns were recorded on a Shimadzu 600° Diffractometer using Cu-Kα radiation (λ=1.5406 A^O) with the voltage of 30 kV and 3° mA at room temperature with the scanning rate of 0.5 degrees per minute. Nitrogen adsorption-desorption measurements were made using Micromeritics ASAP 202° V3.0° H instruments, and the sample was outgassed at 200 ºC for 1 h. The samples' surface areas and pore size were obtained by the Brunauer-Emmett Teller (BET) method. Electron diffraction studies (SEM and TEM) were used to determine the morphology of mesoporous $AlPO_4$-based materials. Scanning Electron Microscope (SEM) images were recorded on a JEOL EO JSM-6390.

2.4 Catalytic reactor

Generally, catalytic activities were carried out in both liquid and vapor phases. The liquid phase trans-esterification of castor oil with ethanol was carried out in a three-necked RB flask with a condenser and a thermometer, as shown in Fig. 1. The weighed amount of ethanol, castor oil and calcined $CuAlPO_4$ and $MgAlPO_4$-based catalysts were added and allowed to stir for the required time.

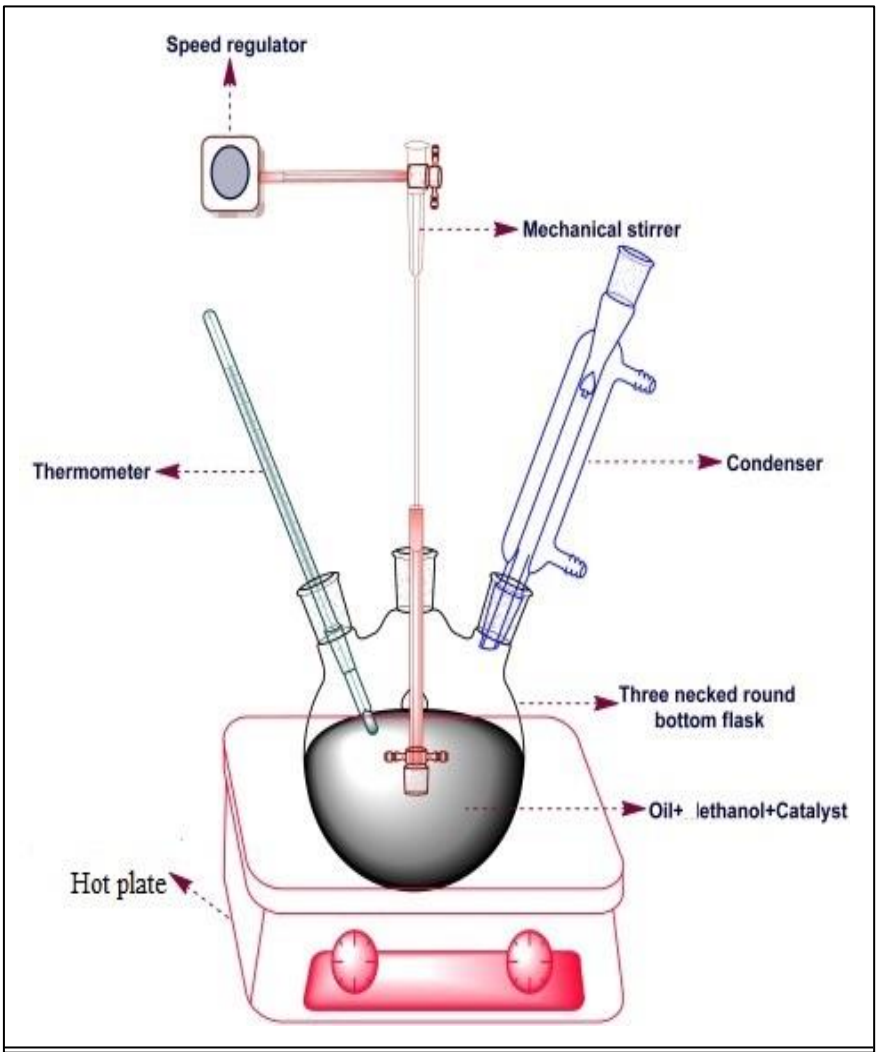

Fig. 1: Reactor setup for Biodiesel synthesis

3. RESULT AND DISCUSSION

3.1 Characterization of $AlPO_4$-based molecular sieves

Characterization techniques were essential to confirm the formation of tetrahedral structure, crystalline nature, surface area and pore size and morphology.

FT-IR

The FT-IR spectra of as-synthesized and calcined mesoporous $AlPO_4$-based materials such as $CuAlPO_4$ and $MgAlPO_4$ are shown in Fig. 2 (a, b, c and d); they revealed a strong and broadband at 3,450 cm^{-1} to 3,550 cm^{-1} which was assigned to the O-H vibration of water molecules present in both the as-synthesized samples. But in the calcinated sample, the strong –OH band became weak. The complete removal of the template was confirmed by the absence of characteristic C-H stretching bands at 2300 cm^{-1} to 2350 cm^{-1} and C-H deformation bands around 1630 cm^{-1} to 1650 cm^{-1}. The strong band at 1073 cm^{-1} was ascribed to the asymmetric stretching mode of tetrahedral $AlPO_4$. The corresponding symmetric stretching was observed at 670 cm^{-1} to 885 cm^{-1}, for both as-synthesized and calcinated samples of $CuAlPO_4$ and $MgAlPO_4$ **(**Campelo *et al.* 2003; 1986; Vijayasankar *et al.* 2010**).** The bending mode was positioned near 480 to 530 cm^{-1} for both the samples.

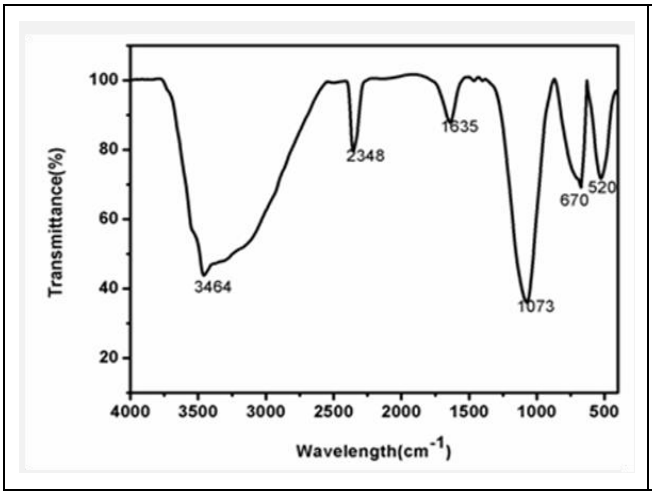

Fig. 2 a: As-synthesized $CuAlPO_4$

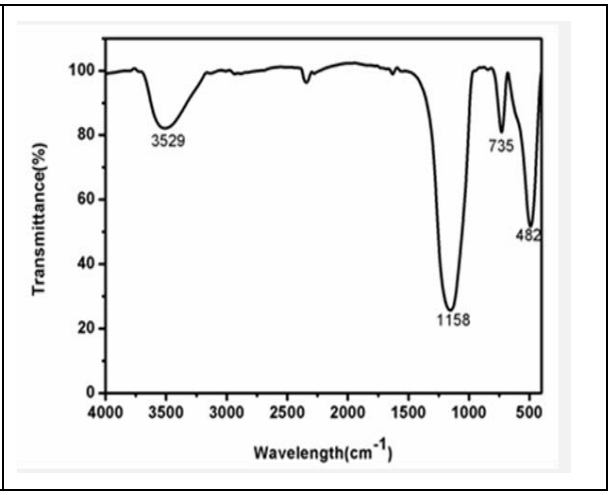

Fig. 2 b: Calcinated $CuAlPO_4$

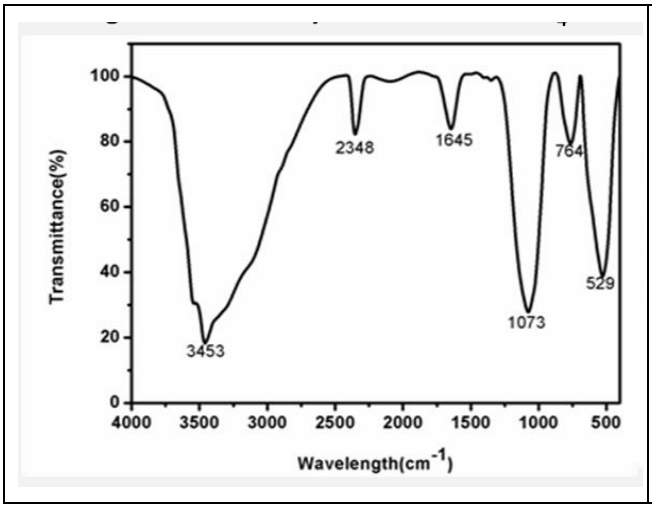

Fig. 2 c: As-synthesized $MgAlPO_4$

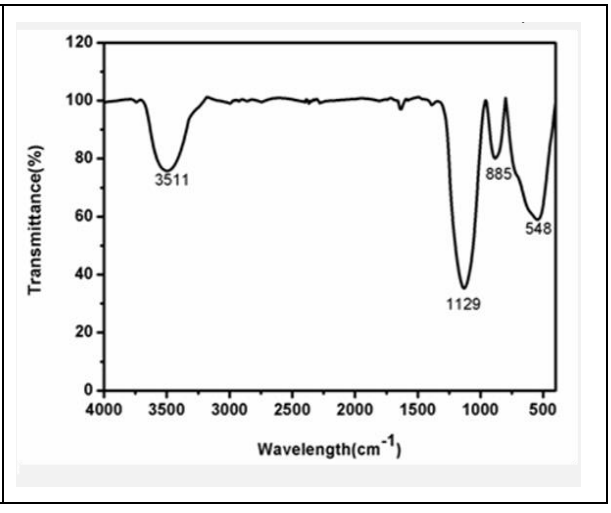

Fig. 2 d: Calcinated $MgAlPO_4$

X-Ray Diffraction

The powder XRD analysis has been carried out for calcinated $MgAlPO_4$ materials (Fig. 3 a and Fig. 3 b). The XRD pattern of calcined $CuAlPO_4$ has an intense high peak at $2\Theta = 21.61^o$ with a d-spacing of 0.41 nm, which proved the well-crystalline nature of the material. Similarly, the XRD pattern of calcined $MgAlPO_4$ has an intense high peak at $2\theta = 66.96^o$ with the d-spacing of 0.13 nm showing high intense reflection. The XRD data were given in the following Table 1.

Table 1. XRD data for $CuAlPO_4$ and $MgAlPO_4$

Metal ion	Ionic Radii	JC-PDF No	Crystal system	Crystal Lattice
iCu^{2+}	0.56	881680	Hexagonal	Primitive
Mg^{2+}	0.54	881680	Hexagonal	Primitive

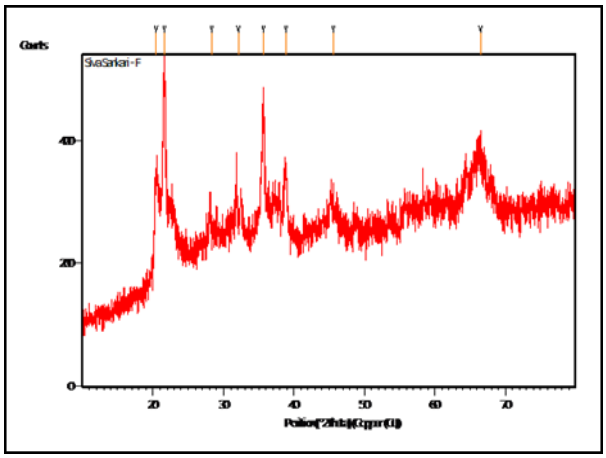

Fig. 3 a: XRD pattern of $CuAiPO_4$

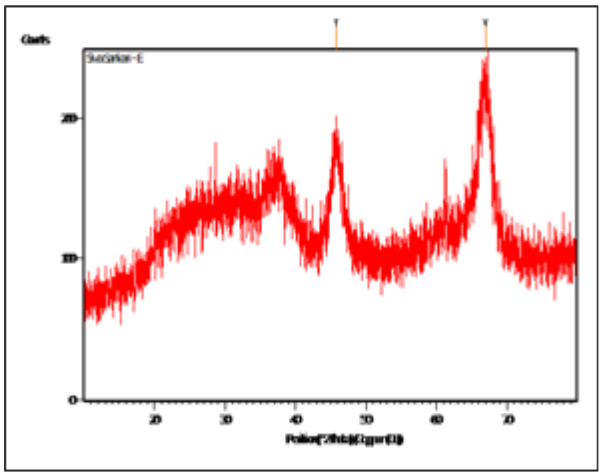

Fig. 3 b: XRD pattern of $MgAlPO_4$

N_2 Adsorption and Desorption Isotherm

The BET surface area and pore volume of the $CuAlPO_4$ were found as 30.13 m^2/g and 0.034, respectively. The pore diameter of $CuAlPO_4$ was 4.47 nm. The BET surface area and pore volume of $MgAlPO_4$ were 71.4° m^2/g and 0.111, respectively. The pore diameter for $MgAlPO_4$ was 6.21 nm. The data proved that $CuAlPO_4$ and $MgAlPO_4$ were mesoporous molecular sieves.

Scanning Electron Microscopy

The morphology of the calcined $CuAlPO_4$ and $MgAlPO_4$ were studied by SEM analysis (Fig. 4 a and Fig. 4 b). SEM images represented the crystalline nature of metal ion-incorporated $AlPO_4$ materials. Both the materials have varied particle sizes in nanoscale. Even though these materials were synthesized by the same synthesis procedure, they were slightly varied for $CuAlPO_4$ and $MgAlPO_4$. The morphological change of $CuAlPO_4$ and $MgAlPO_4$ were with respect to the metal ion incorporation in the tetrahedral framework of the materials (Melo *et al.* 1999). It was evident for the metal ion incorporation in the tetrahedral framework of $AlPO_4$.

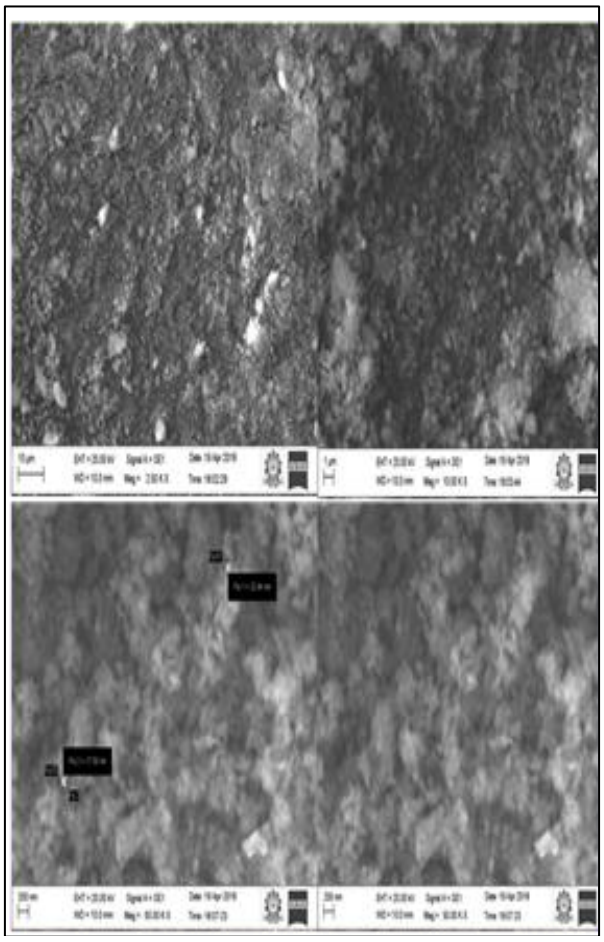

Fig. 4 a: SEM Micrograph $CuAlPO_4$

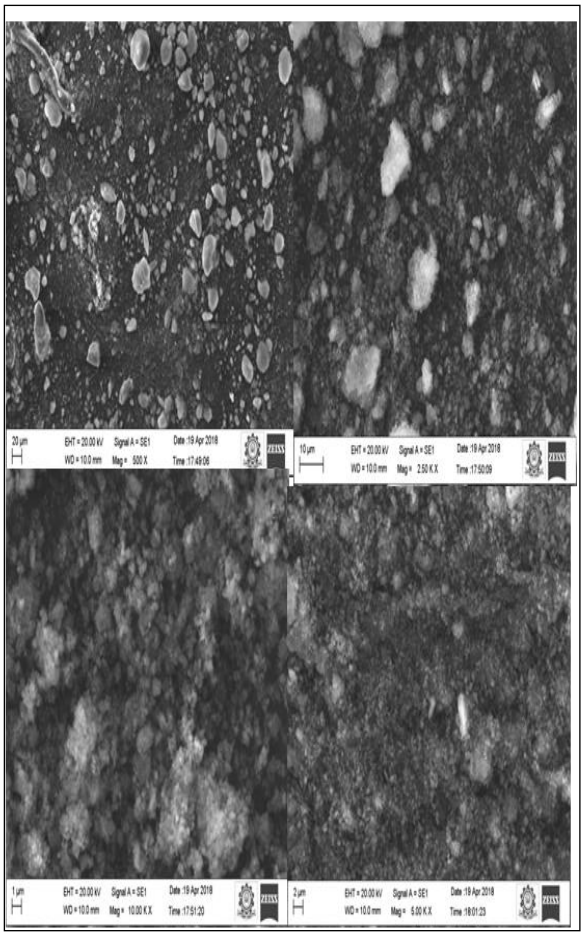

Fig. 4 b: SEM Micrograph $MgAlPO_4$

4. TRANS-ESTERIFICATION OF CASTOR OIL WITH ETHANOL

Molecular sieves

Trans-esterification of castor oil with ethanol has been carried out over the catalysts in the liquid phase. The experimental conditions like the effect of contact time, temperature, catalyst dosage and molar ratio were determined for maximum conversion and selectivity of the reaction.

4.1 Effect of contact time

The effect of contact time on the transesterification of castor oil with ethanol over both the catalyst of $CuAlPO_4$ and $MgAlPO_4$, has been carried out (Table 2 and 3). Fig. 5 shows the effect of contact time on trans-esterification reactions over $CuAlPO_4$ and $MgAlPO_4$ upto 4 h. The percentage of conversion of ethanol increased up to 2 h for $CuAlPO_4$ and 3 h for $MgAlPO_4$, and decreased with further increase in time. The product formed in this reaction was biodiesel, glycerol and diethyl ether.

The selectivity of biodiesel over $CuAlPO_4$ was 81% and $MgAlPO_4$ was 44%. The Cu^{2+} ion present in the tetrahedral framework of the catalyst promoted the maximum trans-esterification reaction than Mg^{2+}ion.

Table 2. Effect of Contact time on Biodiesel synthesis over $CuAlPO_4$

Time (h)	Conversion (%)	Selectivity (%)		
		Biodiesel	Glycerol	Diethyl ether
1	04	06	91	03
2	52	81	14	05
3	06	07	84	08
4	01	02	97	02

Conditions: Catalyst dosage - 0.5 g; Temperature - 50 °C and Molar ratio - 1:3

Table 3. Effect of Contact time on Biodiesel synthesis over $MgAlPO_4$

Time (h)	Conversion (%)	Selectivity (%)		
		Bio - diesel	Glycerol	Diethyl ether
1	12	13	79	09
2	25	31	67	02
3	43	44	53	02
4	05	07	91	02

Conditions: Catalyst dosage - 0.5g; Temperature - 50 °C and Molar ratio - 1:3

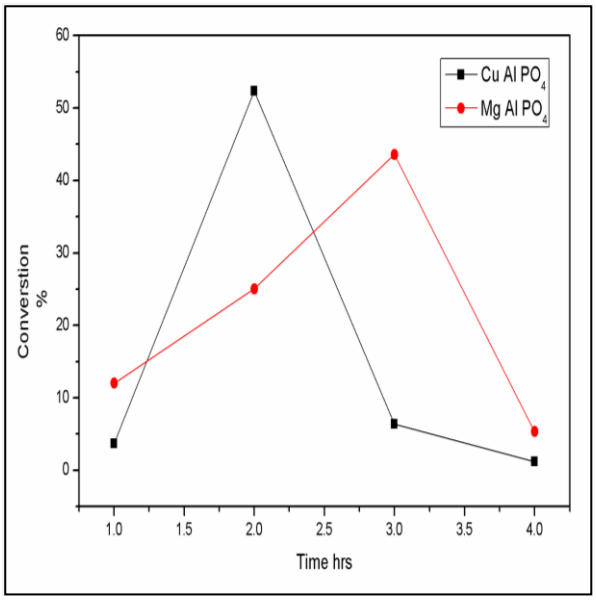

Fig. 5: Effect of Contact time on Biodiesel synthesis

4.2 Effect of Temperature

The percentage conversion of castor oil and selectivity of the products were studied over $CuAlPO_4$ and $MgAlPO_4$. The temperature effect on this reaction were shown in Tables 4 and 5 and Fig. 6.

Table 4. Effect of Temperature on Biodiesel synthesis over $CuAlPO_4$

Temp (°C)	Conversion %	Selectivity (%)		
		Bio diesel	Glycerol	Diethyl ether
Room T	42	74	23	3
50	62	46	43	11
70	22	23	70	8
80	18	41	39	20

Conditions: Catalyst dosage - 0.5 g; Time - 2 h and Molar ratio - 1:3

Table 5. Effect of Temperature on Biodiesel synthesis over $MgAlPO_4$

Temp (°C)	Conversion (%)	Selectivity (%)		
		Bio diesel	Glycerol	Diethyl ether
Room T	17	21	78	01
50	18	23	59	18
70	15	15	69	16
80	9.33	9.80	39.45	7.86

Conditions: Catalyst dosage - 0.5 g; Time - 2 h and Molar ratio - 1:3

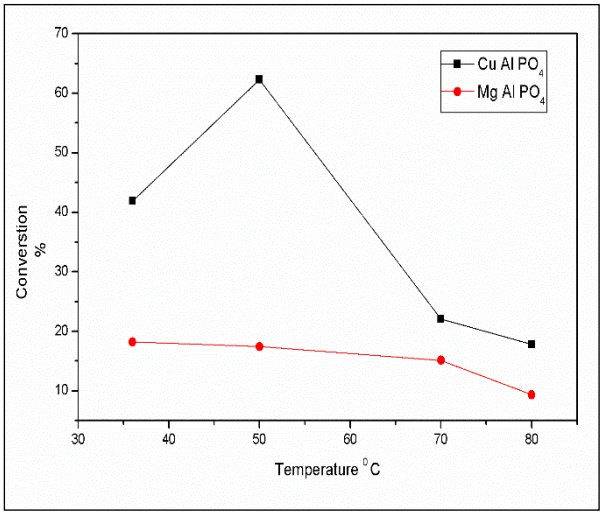

Fig. 6: Effect of Contact temperature on Biodiesel synthesis

4.3 Effect of Mole ratio

The mole ratio effect of castor oil with ethanol over $CuAlPO_4$ and $MgAlPO_4$ catalysts on trans-esterification reaction were studied and shown in Fig. 7. Mole ratio effect on biodiesel synthesis has been studied from 1:2 to 1:4 ratios (castor oil: ethanol). The data were presented in Tables 6 and 7. With the increase of ethanol ratio, castor oil conversion increased upto 1:3 and and decreased with further increase in mole ratio. Selectivity of the biodiesel also increased with an increase of mole ratio upto 1:3 and decreased with further increase in biodiesel selectivity.

Table 6. Effect of Mole ratio on Biodiesel synthesis over $CuAlPO_4$

Mole Ratio	Conversion (%)	Selectivity (%)		
		Biodiesel	Glycerol	Diethyl ether
1:2	06	07	01	92
1:3	52	81	14	05
1:4	01	01	97	01

Conditions: Temperature - 50 °C; Time - 2h and Catalyst dosage - 0.5 g

Table 7. Effect of Mole ratio on Biodiesel synthesis over $MgAlPO_4$

Mole Ratio	Conversion %	Selectivity (%)		
		Bio-diesel	Glycerol	Diethyl ether
1:2	02	20	70	10
1:3	25	31	67	02
1:4	01	02	97	02

Conditions: Temperature - 50 °C; Time - 2h and Catalyst dosage - 0.5 g

4.4 Effect of catalytic dosage

Catalysts used for the conversion and selectivity were studied by increasing the catalyst dosage from 0.5 to 1.5 g. Experimental data were presented in Table 8 and 9 and the effect of trans-esterification was shown in Fig. 8. Conversion of the reaction decreased with an increase in catalytic dosage; however, the biodiesel selectivity decreased with increase in catalytic dosage. But glycerol selectivity increased with increase in catalyst dosage. The mole ratio was fixed as 1:3. The mole ratio was sufficient for producing biodiesel at the catalyst dosage of 0.5 g. When increased, the catalyst dosage cleavage of ester (castor oil) increased. Ethanol also reacted with catalyst to produce ethylene gas. Hence, biodiesel formation decreased with increase of catalytic dosage. It was supported by the selectivity of glycerol. The glycerol selectivity increased with increased catalyst dosage due to the cleavage of the ester linkage. The alcohol was not sufficient for trans-esterification reaction and hence the hydrocarbon chain of the castor oil might have cracked and evolved as the gaseous product. Hence, the

biodiesel conversion decreased with increase in catalyst dosage.

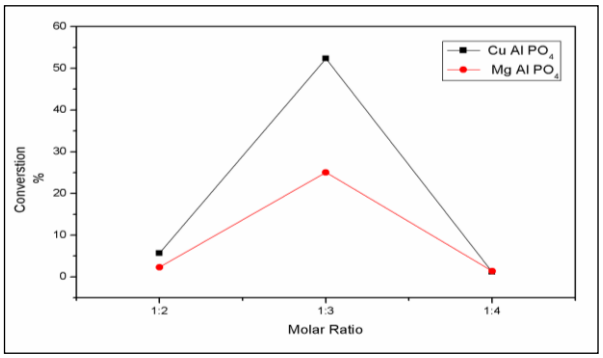

Fig. 7: Effect of Molar ratio on Biodiesel synthesis

Table 8. Effect of Catalytic dosage on Biodiesel synthesis ove $CuAlPO_4$

Catalytic dosage (g)	Conversion %	Selectivity (%)		
		Bio-diesel	Glycerol	Diethyl Ether
0.5	52	81	14	05
1.0	31	39	55	05
1.5	11	23	74	03

Conditions: Temperature - 50 °C; Time - 2 h and Molar ratio - 1:3

Table 9. Effect of Catalytic dosage on Biodiesel synthesis over $MgAlPO_4$

Catalytic dosage (g)	Conversion (%)	Selectivity (%)		
		Biodiesel	Glycerol	Diethyl ether
0.5	25	31	67	02
1.0	13	14	84	02
1.5	06	07	92	01

Conditions: Temperature - 50 °C; Time - 2 h and Molar ratio - 1:3

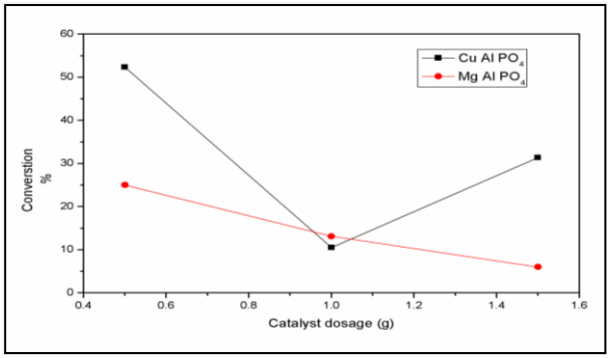

Fig. 8: Effect of Catalytic dosage on Biodiesel synthesis

5. CONCLUSION

Mesoporous $CuAlPO_4$ and $MgAlPO_4$ have been successfully synthesized by adopting simple hydrothermal techniques. These synthesized materials were characterized by FT-IR, XRD, SEM, BET surface area measurements. The FT-IR spectrum has proved the formation of a tetrahedral framework. XRD analysis and SEM images have confirmed the crystalline nature and the morphology of the molecular sieves. BET surface area analysis has revealed the higher surface area and the pore diameter of the porous materials. Thus, the characterization techniques have proved the formation of mesoporous $MgAlPO_4$ and $CuAlPO_4$ molecular sieves. The biodiesel synthesis reaction has been carried out by using ethanol. Conversion and selectivity of biodiesel were more on $CuAlPO_4$ than $MgAlPO_4$.

FUNDING

This research received no specific grant from any funding agency in the public, commercial, or not-for-profit sectors.

CONFLICTS OF INTEREST

The authors declare that there is no conflict of interest.

REFERENCES

Campelo, J. M., Jaraba, M., Luna, D., Luque, R., Marinas, J. M. and Romero, A. A., Effect of phosphate precursor and organic additives on the structural and catalytic properties of amorphous mesoporous $AlPO_4$ materials, *Chem. Mater*., 15(17), 3352-3364 (2003). https://dx.doi.org/10.1021/cm030206+

Campelo, J. M., Marinas, J. M., Mendioroz, S. and Pajares, J. A., Texture and surface chemistry of aluminium phosphates, *J. Catal*., 101(2), 484-495 (1986). https://dx.doi.org/10.1016/0021-9517(86)90275-7

Cheralathan, K., Kannan, C., Palanichamy, M. and Murugesan, V., Ethylation of tolyene over aluminophosphate based molecular sieves in the vapour phase, *Ind. J. Chem. Technol*., *39A*:921-927 (2000).

Elangovan, S. P., Kannan, C., Arabindoo Banumathi and Murugesan, V., Aniline methylation over AFI and AEL type molecular sieves, *Applied Catalysis A: General*, 174(1-2), 213-219 (1998). https://dx.doi.org/10.1016/S0926-860X(98)00189-6

Jing Yu, Anjie Wang, Xiang Li, Juan Tan, Yongkang Hu, An improved calcinations route to obtain high quality mesoporous aluminophosphates materials, *Mater. Lett.*, 61(13), 2620-2623 (2007). https://dx.doi.org/10.1016/j.matlet.2006.10.009

Melo, A. A. Rogerio, Giotto, M. V., Rocha, J. and Urquieta Gonzalez, E. A., MCM-41 ordered mesoporous molecular sieves synthesis and characterization, Mater. *Res*., 2(3), 173-179 (1999). https://dx.doi.org/10.1590/S1516-14391999000300010

Selvam, P. and Mohapatra, S. K., Thermally stable trivalent iron-substituted hexagonal mesoporous aluminophosphate (FeHMA) molecular sieves: Synthesis, characterization and catalytic properties, J. *Catal.*, 238(1), 88-99 (2006). https://dx.doi.org/10.1016/j.jcat.2005.12.005

Subrahmanyam, Ch., Louis, B., Rainone, F., Viswanathan, B., Renken, A. and Varadarajan, T. K., Catalytic oxidation of toluene with molecular oxygen over Cr-substituted mesoporous materials, *Applied catalysis A: General*, 241(1-2), 205-215 (2003). https://dx.doi.org/10.1016/S0926-860X(02)00469-6

Tatsuo Kimura, Surfactant – template mesoporous aluminophosphate – based materials and the recent progress, *Microporous Mesoporous Mater.*, 77:97-107 (2005). https://dx.doi.org/10.1016/j.micromeso.2004.08.023

Vijayasankar, A. V., Mahadevaiah, N., Bhat, Y. S. and Nagaraju, N., Mesoporous aluminophosphate materials: influence of method of preparation and iron loading on textural properties and catalytic activity, *J. Porous Mater*., 18(3), 369-378 (2011). https://dx.doi.org/10.1007/s10934-010-9387-z